

# Formation of brownmillerite type calcium ferrite ( $\text{Ca}_2\text{Fe}_2\text{O}_5$ ) and catalytic properties in propylene combustion

Daisuke Hirabayashi,<sup>a,\*</sup> Takeshi Yoshikawa,<sup>a</sup> Kazuhiro Mochizuki,<sup>a</sup> Kenzi Suzuki,<sup>a</sup> and Yoichi Sakai<sup>b</sup>

<sup>a</sup>*EcoTopia Science Institute, Nagoya University, Nagoya 464-8603, Japan*

<sup>b</sup>*Department of Chemistry, Daido Institute of Technology, Nagoya 457-8530, Japan*

Received 15 February 2006; accepted 1 June 2006

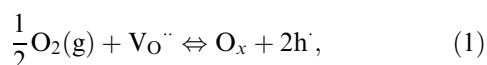
Several types of calcium ferrite base catalysts ( $\text{Ca}/\text{Fe} = 0.33\text{--}3$ ) for propylene ( $\text{C}_3\text{H}_6$ ) combustion were prepared. Calcium ferrite catalyst with brownmillerite crystal structure provided catalytic activity for  $\text{C}_3\text{H}_6$  combustion in the temperature range of 250–450 °C. The brownmillerite phase ( $\text{Ca}_2\text{Fe}_2\text{O}_5$ ) was responsible for the formation of oxygen adspecies ( $\text{O}_2^-$ ) in the surface layer below 450 °C.

**KEY WORDS:** brownmillerite; calcium ferrites; superoxide.

## 1. Introduction

In recent years, the treatment of volatile organic compounds (VOCs) has attracted scientists' attention from various fields. In particular, catalytic combustion in the presence of oxidation catalysts has been shown to be a promising method for the destruction of the toxic chemicals [1,2]. Noble metal based catalysts, such as platinum and palladium have been regarded as a desirable, due to high activity for the destruction of polluting materials [3–9]. The several transition-metal based catalysts (e.g.  $\text{CoO}$ ,  $\text{CuO}$ ) shows relatively high activity, but a large consumption of these metals would be desirable environmentally due to the toxicity.

Perovskite type oxides (figure 1a) are also candidates for VOCs combustion and are possible alternative oxidation catalysts and catalysts supports [10–13]. The structure permits accommodation of a wide variety of metal cations of different valences and has an unusual capacity to support a number of different types of defects. Depending on the composition, these structures provide important properties in the catalytic oxidation such as high electronic electron–hole and oxide-ion conductivity and the capacity of the conductive oxide ions. The oxide ions can be formed by the oxygen-exchange reaction between oxygen and the oxygen vacancies in the crystal lattice:



where  $\text{V}_{\text{O}}^{\bullet\bullet}$  represents oxygen vacancy included in the structure,  $\text{O}_x$  oxide ion at normal lattice site,  $\text{h}$  electron hole. Thus, it was considered that the defects in the perovskite structures strongly affect the formation of the conductive oxide ions as well as their catalytic activities. Catalytic combustion of  $\text{C}_3\text{H}_6$  and other VOCs over perovskite-type oxides has been studied for decades, however there has been little attention on brownmillerite-type calcium ferrite for the same purpose. The brownmillerite structure ( $\text{Ca}_2\text{Fe}_2\text{O}_5$ , figure 1b) has an orthorhombic crystal, which is composed of a three-dimensional framework of corner-sharing  $\text{FeO}_6$  octahedron and  $\text{FeO}_4$  tetrahedron with two oxygen vacancies ( $\text{V}_{\text{O}}^{\bullet\bullet}$ ). Accordingly, the brownmillerite structure should stabilize the oxygen defects which provide active sites for oxygen exchanging. The structure was investigated as a non-stoichiometric cubic perovskite which has originally includes anionic defects without doping other rare-earth metals. Several phases formulated  $\text{CaFe}_{1-y}^{3+}\text{Fe}_y^{4+}\text{O}_{3-(1-y)/2}$  have been characterized depends on the way in which the compounds have been prepared (thermal treatment, nature of the starting materials, co-crystallization with other compounds) [14–16].

In this work, we examine the activity for  $\text{C}_3\text{H}_6$  combustion over brownmillerite calcium ferrites ( $\text{Ca}_2\text{Fe}_2\text{O}_5$ ) and related calcium ferrites without using toxic materials and costly noble metals. The formation of brownmillerite crystal structure at different  $\text{Ca}/\text{Fe}$  mixing ratio and the active species on the surface of the brownmillerite calcium ferrite for  $\text{C}_3\text{H}_6$  combustion are discussed.

\*To whom correspondence should be addressed.  
E-mail: hirabayashi@esi.nagoya-u.ac.jp

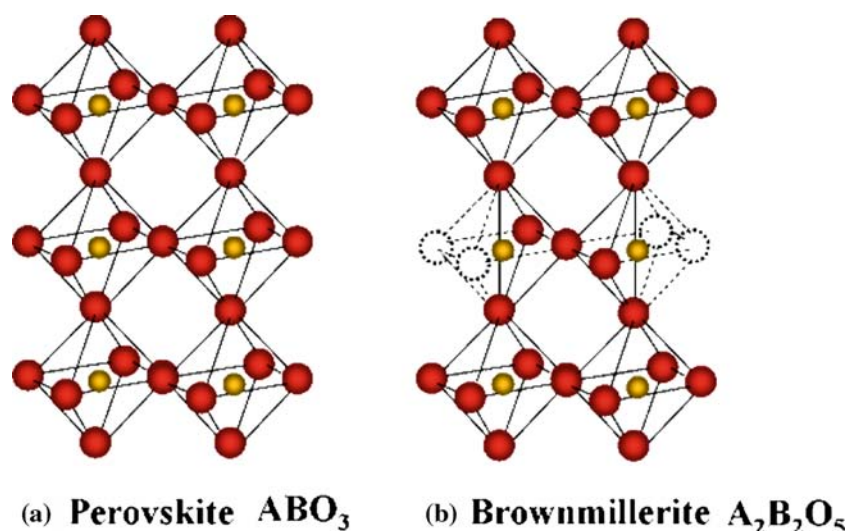


Figure 1. Perovskite  $ABO_3$  and brownmillerite  $A_2B_2O_5$  type structures ( $A = \text{Ca}$ ,  $B = \text{Fe}$  for  $\text{Ca}_2\text{Fe}_2\text{O}_5$ ). B cations are shown as yellow spheres in 6- or 4-coordinations with oxygen atoms (red spheres).

## 2. Experimental

Calcium ferrites powders were prepared by ceramic route by physically mixing an appropriate ratio of  $\text{CaO}$  and  $\text{Fe}_2\text{O}_3$  at different mixing ratios ( $\text{Ca}/\text{Fe} = 0.33\text{--}3$ ) and calcining the mixture at  $1000^\circ\text{C}$  for 3 h in air. The X-ray powder diffraction patterns were obtained with a diffractometer (RIGAKU, RINT-TTR) using  $\text{CuK}\alpha$  radiation (50 kV, 100 mA).  $^{57}\text{Fe}$ -Mössbauer measurements were performed at 293 K in an ordinary mode, using spectrometers fabricated by Topologic Systems, Inc. The isomer shift and Doppler velocity scale were calibrated with respect to metallic iron at 293 K. The Raman spectroscopy experiments was carried out using a spectrometer with the 532 nm line of green laser for excitation (JASCO, NRS-1000), and about 100 mW of power was focused on the sample powders.

The combustion of  $\text{C}_3\text{H}_6$  was performed using a conventional fixed-bed reactor of quartz glass in the temperature range from 100 to  $900^\circ\text{C}$ . The concentration of  $\text{C}_3\text{H}_6$  was 1000 ppmv. By mixing helium carrier with oxygen (90 vol%  $\text{He}$ , 10 vol%  $\text{O}_2$ ), the flow rate was controlled to be  $30\text{ ml min}^{-1}$  corresponding to a space velocity of *ca.*  $9500\text{ h}^{-1}$ . The calcium ferrite powders were sieved to under  $100\text{ }\mu\text{m}$  in particle size and put into the reactor between glass wools for packing and support. Analysis of the effluent gases was performed using an FID gas chromatograph (Shimazu, GC-8A). The specific surface area was measured using an  $\text{N}_2$  adsorption-desorption equipment at 77 K (Bell Japan, BELSORP-28SP).

Temperature programmed reduction ( $\text{H}_2$ -TPR) and oxygen desorption/sorption measurements were carried out in a thermogravimetric analyzer (Shimazu, TGA-50). For  $\text{H}_2$ -TPR experiments, about 10 mg sample was loaded in a Pt cell in the TGA. The sample was first treated under flowing oxygen gas at  $800^\circ\text{C}$  for 1 h,

cooled down to  $100^\circ\text{C}$  under the same atmosphere, and reduced ( $50\text{ ml min}^{-1}$ ). The temperature increased from 100 to  $1000^\circ\text{C}$  at a rate of  $5^\circ\text{C min}^{-1}$ . For oxygen desorption/sorption measurements, the powders of calcium ferrites were reduced under 5 vol%  $\text{H}_2$  at  $450^\circ\text{C}$  and remained at this temperature during the analysis, followed by introduction of a pure  $\text{O}_2$  ( $50\text{ ml min}^{-1}$ ) to the powders (*ca.* 10 mg) dispersed on the Pt cell. The storage/release amount of oxygen [ $\mu\text{mol/g}$ ] was calculated from the difference (gain/loss) between the initial and final weight balanced in each flows.

## 3. Results and discussion

### 3.1. X-ray Diffraction patterns

Upon calcination of a mixture of  $\text{CaO}$  and  $\text{Fe}_2\text{O}_3$  powders at  $1000^\circ\text{C}$ , the mixture transforms to mainly two calcium ferrites ( $\text{Ca}_2\text{Fe}_2\text{O}_5$  and  $\text{CaFe}_2\text{O}_4$ ) according to the following equations.

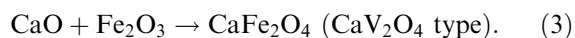
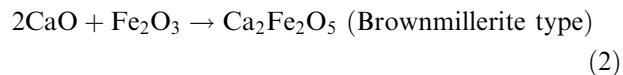


Figure 2 shows powder XRD patterns of the reaction products from the mixture of  $\text{CaO}$  and  $\text{Fe}_2\text{O}_3$  with different  $\text{Ca}/\text{Fe}$  ratio. It was clearly found that there was a drastic change of crystal phases with decreasing  $\text{Ca}/\text{Fe}$  atomic ratio. The  $\text{Ca}(\text{OH})_2$  (formed from the  $\text{CaO}$  phase by hydration with atmospheric moisture after the reaction, marked by open circle) disappeared and then the brownmillerite-type  $\text{Ca}_2\text{Fe}_2\text{O}_5$  phases (closed triangle) changed to the  $\text{CaV}_2\text{O}_4$  type  $\text{CaFe}_2\text{O}_4$  phase (open triangle). Here, the most clear peaks assigned to  $\text{Ca}_2\text{Fe}_2\text{O}_5$  were observed at  $\text{Ca}/\text{Fe} = 1$ , although small peaks for

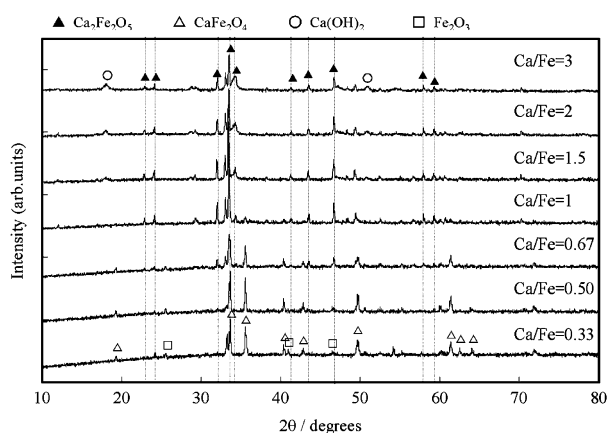


Figure 2. X-ray diffraction patterns of calcium ferrites prepared from the mixture of CaO and Fe<sub>2</sub>O<sub>3</sub> with atomic Ca/Fe ratio between 0.33 and 3.

CaFe<sub>2</sub>O<sub>4</sub> and Ca(OH)<sub>2</sub> remain in the pattern. Similarly, the strongest peaks for CaFe<sub>2</sub>O<sub>4</sub> were found at Ca/Fe = 0.5. In this case, clear peaks assigned to Ca<sub>2</sub>Fe<sub>2</sub>O<sub>5</sub> were not detected in the pattern.

### 3.2. <sup>57</sup>Fe-Mössbauer spectra

Typical <sup>57</sup>Fe-Mössbauer spectra measured at 293 K for calcium ferrites are shown in Figure 3, where the mixing atomic ratios (Ca/Fe) in the starting mixtures are 0.33, 1, and 3. Analysis of the Mössbauer spectra revealed that a main product in the samples with Ca/Fe = 0.33 and 1.00 was brownmillerite type Ca<sub>2</sub>Fe<sub>2</sub>O<sub>5</sub> with two ferric ion (III) sites of tetrahedral and octahedral coordination (see figure 1b), however, the iron site containing ferric ion (IV) were not detected at room temperatures. Calcium ferrite (Ca/Fe = 1) appeared in the spectra of figure 3 as two sets of sextet with an almost identical intensity, although their absorptions

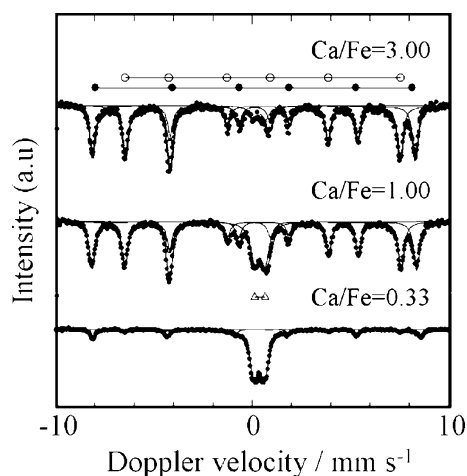


Figure 3. <sup>57</sup>Fe-Mössbauer spectra of calcium ferrites prepared from the mixture of CaO and Fe<sub>2</sub>O<sub>3</sub> with atomic ratio Ca/Fe = 0.33 (bottom), 1 (middle) and 3 (top).

were too weak for the Ca/Fe = 0.33 sample. The two sextets are indicated by the markers in the figure, where closed and open circles set for Fe<sup>3+</sup> occupied at octahedral (FeO<sub>6</sub>) and tetrahedral (FeO<sub>4</sub>) sites, respectively. For the brownmillerite-type structure, the isomer shift, quadrupole splitting, internal field were evaluated to be 0.35 mm s<sup>-1</sup>, -0.52 mm s<sup>-1</sup>, and 50.7 T for the octahedral site and 0.18 mm s<sup>-1</sup>, 0.72 mm s<sup>-1</sup> and, 43.2 T for the tetrahedral site. Mössbauer parameters at 293 K agree with those at 300 K previously reported by Randhawa and Sweetz [17]. These authors reported Mössbauer parameters of 0.37 mm s<sup>-1</sup>, -0.52 mm s<sup>-1</sup>, and 50.4 T for the octahedral site, and 0.18 mm s<sup>-1</sup>, 0.72 mm s<sup>-1</sup> and, 42.9 T for the tetrahedral site of Ca<sub>2</sub>Fe<sub>2</sub>O<sub>5</sub>.

XRD (figure 2) and Fe-Mössbauer (figure 3) results suggest that the calcination of a CaO and Fe<sub>2</sub>O<sub>3</sub> mixture in air at 1000 °C results in the formation of crystalline phases of Ca<sub>2</sub>Fe<sub>2</sub>O<sub>5</sub> and/or CaFe<sub>2</sub>O<sub>4</sub>. The brownmillerite-type Ca<sub>2</sub>Fe<sub>2</sub>O<sub>5</sub> phase was formed at Ca/Fe > 0.33. As the mixing atomic ratio was increased, the diffraction peaks became narrower and higher due to the crystal growth of Ca<sub>2</sub>Fe<sub>2</sub>O<sub>5</sub>. In this case, the Mössbauer absorption area (which corresponded to the product yields of Ca<sub>2</sub>Fe<sub>2</sub>O<sub>5</sub>) increased. The most pronounced change in the Mössbauer absorption spectra resulted from a mixing atomic ratio of 1, where the products yield of Ca<sub>2</sub>Fe<sub>2</sub>O<sub>5</sub> calculated from adsorption was about 75%.

### 3.3. Raman spectra

A very attractive feature of perovskite related compounds is the formation of active oxygen adspecies over the surface. Figure 4(a), (b) shows the Raman spectra of the powders after preparation at room temperature. The spectra were scanned in the range of 1200–850 cm<sup>-1</sup>

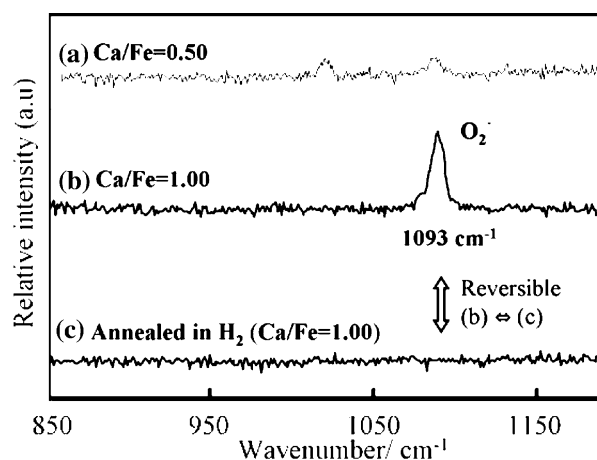
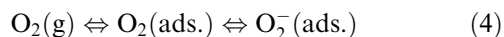


Figure 4. Raman spectra of calcium ferrites prepared from the mixture of CaO and Fe<sub>2</sub>O<sub>3</sub> with atomic ratio Ca/Fe = 1; (b) and 0.5; (a), and spectrum (c) of calcium ferrite at Ca/Fe = 1 after annealing under H<sub>2</sub> flow at 500 °C.

with a resolution of  $2\text{ cm}^{-1}$ . According to Raman spectroscopic datum of the sample at  $\text{Ca/Fe} = 1$ ; (b), an intense absorption at  $1093\text{ cm}^{-1}$  is observed. This absorption has typically been assigned to the superoxide radical ( $\text{O}_2^-$ ) in this region. Molecular  $\text{O}_2$  species has been assigned to a band at *ca.*  $1556\text{ cm}^{-1}$ ; the superoxide radical ( $\text{O}_2^-$ ) is observed to have a stretching vibration frequency at  $1180\text{ cm}^{-1}$  on  $\text{TiO}_2$  [18] and at  $1160\text{--}1015\text{ cm}^{-1}$  on  $\text{MgO-CoO}$  [19,20], mayenite type aluminum silicate [21–23] has been typically found an absorption in a broad range ( $640\text{--}970\text{ cm}^{-1}$ ). Spectra at  $\text{Ca/Fe} = 0.50$ ; (a) also exhibited two weak shifts at  $1022$  and  $1092\text{ cm}^{-1}$ , however the former shift was less definitive. Figure 4(c) shows the Raman spectrum of calcium ferrite powders ( $\text{Ca/Fe} = 1$ ) after annealing in  $\text{H}_2$  flow at  $500^\circ\text{C}$ . As can be seen, absorption due to superoxide radicals ( $\text{O}_2^-$ ) almost disappeared after annealing. Moreover, the absorption at  $1093\text{ cm}^{-1}$  appeared reversibly after the annealing in air flow for 6 h at  $500^\circ\text{C}$ , although the intensity of the absorption was reduced. The above results suggest that the following adsorption equilibrium between  $\text{O}_2/\text{O}_2^-$  may exist on the surface of brownmillerite type  $\text{Ca}_2\text{Fe}_2\text{O}_5$  under an air atmosphere.



### 3.4. Catalytic activity

We examined the catalytic activity of the prepared calcium ferrites. Figure 5 (the light-off curves) summarizes the results. For all the prepared catalysts,  $\text{C}_3\text{H}_6$  conversion increased with the elevation of reaction temperature. The  $\text{C}_3\text{H}_6$  combustion started around  $150$ ,  $180$ ,  $200$ ,  $210$ ,  $300$  and  $320^\circ\text{C}$ , and completed around  $180$ ,  $500$ ,  $600$ ,  $610$ ,  $700$  and  $720^\circ\text{C}$  for  $\text{Pt/Al}_2\text{O}_3$ ,  $\text{Ca}_2\text{Fe}_2\text{O}_5$ ,  $\text{CaFe}_2\text{O}_4$  ( $\text{Ca/Fe} = 2$ ),  $\text{Ca}_2\text{Fe}_2\text{O}_5$  with  $\text{CaO}$  ( $\text{Ca/Fe} = 0.5$ ),  $\text{Fe}_2\text{O}_3$  and  $\text{CaO}$ , respectively. Pure  $\text{CaO}$  and  $\text{Fe}_2\text{O}_3$  only showed low activities under the condi-

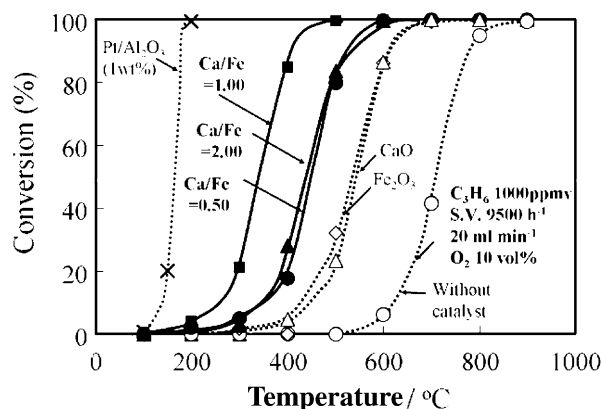


Figure 5. Catalytic activity of calcium ferrites prepared from a mixture of  $\text{CaO}$  and  $\text{Fe}_2\text{O}_3$  with atomic ratio  $\text{Ca/Fe} = 0.5, 1$  and  $2$ .

tions of  $10\text{ vol}\% \text{ O}_2$  and  $\text{GHSV} = 9500\text{ h}^{-1}$ . After calcination of both pure oxides with different mixing ratio, the activities, especially for the calcium ferrites at  $\text{Ca/Fe} = 1$  were found to be apparently improved resulting in a decrease in the reaction temperature (*ca.*  $350^\circ\text{C}$  for  $\text{Ca/Fe} = 1$ ) compared with the same conversion without catalyst. The promoting effect increased according to the sequence of  $\text{CaO} < \text{Fe}_2\text{O}_3 < < \text{Ca}_2\text{Fe}_2\text{O}_5$  with  $\text{CaO}$  ( $\text{Ca/Fe} = 0.5$ )  $< \text{CaFe}_2\text{O}_4$  ( $\text{Ca/Fe} = 2$ )  $< < \text{Ca}_2\text{Fe}_2\text{O}_5$  ( $\text{Ca/Fe} = 1$ )  $< < \text{Pt/Al}_2\text{O}_3$ , where the light-off temperatures defined as the temperature at  $50\%$  in conversion were *ca.*  $540$ ,  $520$ ,  $450$ ,  $430$ ,  $340$  and  $190^\circ\text{C}$ , respectively. Accordingly, these results indicated that the existence of the brownmillerite type  $\text{Ca}_2\text{Fe}_2\text{O}_5$  played significant promoting roles for  $\text{C}_3\text{H}_6$  combustion as an oxidation catalyst. The above results also suggested that the catalytic activity of  $\text{Ca}_2\text{Fe}_2\text{O}_5$  is correlated with the superoxide  $\text{O}_2^-$  formation on the surface of catalysts. The light-off curves also show a higher activation energy of  $\text{Pt/Al}_2\text{O}_3$  than those of any other calcium ferrites. The conversion of  $\text{Pt/Al}_2\text{O}_3$  was increased more quickly with the increase in temperature, indicates that the reaction pathway on the  $\text{Pt/Al}_2\text{O}_3$  is different from that on calcium ferrites samples. The reaction rates on the calcium ferrite may be more strongly affected by diffusion process. A small amount of oxygen species formed on active ferric ion sites would slowly diffuse in the surface or the surface layer, and participated into the reaction.

### 3.5. Oxygen sorption/desorption property

Figure 6 shows the temperature programmed reduction ( $\text{H}_2\text{-TPR}$ ) from calcium ferrite prepared with an atomic  $\text{Ca/Fe}$  ratio of  $1$  and  $0.5$ , in which the ordinate (differential weight changes calculated from TG signal) corresponds to the rate of iron reduction accompanied with oxygen desorption from the calcium ferrites in a

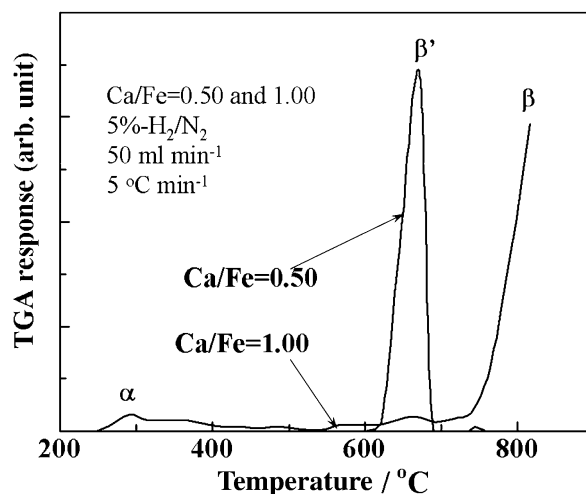


Figure 6. TPR- $\text{H}_2$  spectrum of calcium ferrite prepared from a mixture of  $\text{CaO}$  and  $\text{Fe}_2\text{O}_3$  with atomic ratio  $\text{Ca/Fe} = 1$  and  $0.5$ .

5%  $\text{H}_2/\text{N}_2$ . For the calcium ferrite at  $\text{Ca}/\text{Fe} = 0.5$ , no peak was observed below 500 °C, and only a  $\beta$ -type peak ( $\beta'$ ) was observed at high temperature region (660 °C), indicates the direct reduction of  $\text{Fe}^{3+}$  to  $\text{Fe}^{2+}$ . Similar peak assigned to the reduction to  $\text{FeO}$  was observed in the bulk  $\text{Fe}_2\text{O}_3$  [24]. For  $\text{Ca}/\text{Fe} = 1$ , the  $\text{H}_2$ -TPR result shows a small peak ( $\alpha$ ) at 300 °C and a large peak ( $\beta$ ) over 800 °C, indicated the presence of two types of the active site on  $\text{Ca}_2\text{Fe}_2\text{O}_5$ . Notably, the small peak ( $\alpha$ ) was observed at much lower temperature compared with that of the iron reduction from  $\text{Fe}^{3+}$  to  $\text{Fe}^{2+}$  ( $\beta'$ , 660 °C) and that of the reduction of pure  $\text{Fe}_2\text{O}_3$  to  $\text{Fe}_3\text{O}_4$  (430 °C in ref. [25]). The small peak ( $\alpha$ ) would be related to a reduction of a small amount of  $\text{Fe}^{4+}$  which releases oxygen species at lower temperature as observed for non-stoichiometric Fe-containing perovskites [26].  $\text{Fe}^{4+}$  were observed in brownmillerite type oxide prepared in air, and always present even after annealing in  $\text{Ar}/\text{N}_2$  atmosphere at 1000 °C [27]. It can be considered that the  $\text{C}_3\text{H}_6$  oxidation proceeds at lower temperature on the abnormal valence iron, and that the abnormal valence site provides the oxygen adspecies such as superoxide ( $\text{O}_2^-$ , shown in figure 4) on the  $\text{Ca}_2\text{Fe}_2\text{O}_5$  surface. The latter peaks at high temperature ( $\beta$ ) can be assigned to the reduction of  $\text{Fe}^{3+}$  which corresponds to the release of lattice oxygen ( $\text{O}_x$ ) from the perovskite type ferric iron site ( $\text{FeO}_6$ ). The oxide ions seem to be formed by the oxygen exchange between oxygen and oxygen vacancies ( $\text{V}_{\text{O}}^{\bullet}$ ) on the surface. These oxygen species may involve other higher temperature reaction. The peak areas in TPR spectra can be related to the density of the active sites. The results indicated that the density of  $\text{Fe}^{3+}$  site was much more than that of  $\text{Fe}^{4+}$  density in calcium ferrite at  $\text{Ca}/\text{Fe} = 1$ , indicated that the preparation under reducing or oxidizing condition results in significant difference in the catalytic activity. The peak area of  $\text{Fe}^{4+}$  was very small, and the molar concentration of  $\text{Fe}^{4+}$  was as lower as 2% of total amount of iron ideally included in stoichiometric brownmillerite crystals.

Figure 7 presents the oxygen sorption/desorption behavior of the calcium ferrites powder ( $\text{Ca}/\text{Fe} = 1$ ) at 450 °C. The integrated sorption/desorption amount of oxygen estimated from the total weight change is also given in figure 7. It was observed that the amount of oxygen included in the calcium ferrites is decreased in a 5%  $\text{H}_2/\text{N}_2$  flow, and then the amount was increased in the  $\text{O}_2$  flow with time on stream. The sorption/desorption amount completely recovered to the initial value after saturation with  $\text{O}_2$ . The observed oxygen sorption/desorption amounts at 450 °C ( $83 \mu\text{mol g}^{-1}$ ) corresponded to only *ca.* 6% of total oxygen contents calculated from the total amount of oxygen vacancies in the bulk  $\text{Ca}_2\text{Fe}_2\text{O}_5$  crystal, however the value was larger than that calculated for monolayer sorption capacity of  $\text{O}_2$  ( $40 \mu\text{mol g}^{-1}$ ). In each steps, the oxygen sorption/desorption proceeded slowly on the surface layer.

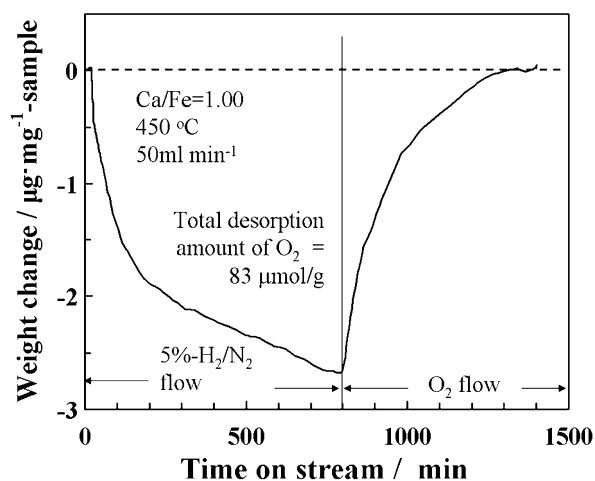


Figure 7. Oxygen desorption/sorption behaviour of calcium ferrite prepared with atomic ratio  $\text{Ca}/\text{Fe} = 1$ .

Namely, the active oxygen species over the  $\text{Ca}_2\text{Fe}_2\text{O}_5$  crystals was slightly released, slowly consumed in the  $\text{H}_2/\text{N}_2$  mixture flow, and then replenished by sorption onto the crystal surface in  $\text{O}_2$  flow. These results indicated that not only adspecies but also a small amount of bulk oxygen in the surface layer could participate to the catalysis.

In summary, the results shows that the redox cycles of brownmillerite phase with high oxygen deficiencies coming from the crystal structure can participate into the  $\text{C}_3\text{H}_6$  oxidation due to a presence of easily reducible iron  $\text{Fe}^{4+}$  sites forming highly active oxygen species at lower temperature compared with a transition metal based catalyst such as  $\text{Fe}_2\text{O}_3$ . In the case of calcium ferrite samples synthesized at  $\text{Ca}/\text{Fe} = 1$ , such brownmillerite make it possible to promote combustion at temperatures above 180 °C, which may be significant interesting for applications to low-cost catalyst and catalyst supports. However, it should also be noted that further studies are necessary to improve the combustion activity of  $\text{Ca}_2\text{Fe}_2\text{O}_5$ , and to assess active sites in the brownmillerite type  $\text{Ca}_2\text{Fe}_2\text{O}_5$  in detail. In addition, the formation of the oxygen species at the abnormal cation sites on the  $\text{Ca}_2\text{Fe}_2\text{O}_5$  surface would significantly promote a catalytic activity of a very small amount of metal-based catalysts ( $\sim 0.1\%$  by weight) which was dispersed on the  $\text{Ca}_2\text{Fe}_2\text{O}_5$  as a support. This attempt may be particularly useful and interesting.

#### 4. Conclusions

In the current study, reasonable and environmentally friendly calcium ferrite based catalysts were synthesized by solid state reaction of the mixture of  $\text{CaO}$  and  $\text{Fe}_2\text{O}_3$  powders with mixing atomic ratio from 0.33 to 3 at 1000 °C. The prepared calcium ferrite catalysts contained mainly two calcium ferrite phases (brownmillerite type  $\text{Ca}_2\text{Fe}_2\text{O}_5$  and  $\text{CaV}_2\text{O}_4$  type  $\text{CaFe}_2\text{O}_4$ ). The

brownmillerite type crystal phase grew at  $\text{Ca/Fe} > 1$ . The clear  $^{57}\text{Fe}$ -Mössbauer absorption assigned to two ferric ion sites of octahedral ( $\text{FeO}_6$ ) and tetrahedral ( $\text{FeO}_4$  with oxygen vacancies) in brownmillerite structure were successfully observed in the spectra at  $\text{Ca/Fe} > 1$ , and the product yield of  $\text{Ca}_2\text{Fe}_2\text{O}_5$  calculated from Mössbauer absorption was  $\sim 75\%$  at  $\text{Ca/Fe} = 1$ . A highly active superoxide radical ( $\text{O}_2^-$ ) could be formed on the surface of calcium ferrites and the atmospheric oxygen strongly affected the equilibrium formation of such oxygen adspecies. The formation of the brownmillerite type  $\text{Ca}_2\text{Fe}_2\text{O}_5$  significantly promote the catalytic combustion of  $\text{C}_3\text{H}_6$  in the temperature range between 250 and 450 °C. The light-off temperature of calcium ferrite at  $\text{Ca/Fe} = 1$  ( $\text{Ca}_2\text{Fe}_2\text{O}_5$ ) was 150 °C higher than that of  $\text{Pt/Al}_2\text{O}_3$  and 180 °C lower than that of  $\text{Fe}_2\text{O}_3$ , and the combustion started at 90–140 °C lower temperature than those obtained using other calcium ferrites ( $\text{Ca/Fe} = 0.5, 2$ ). The promoting effects of the combustion can be ascribed to the activation of oxygen adspecies (such as  $\text{O}_2^-$ ), which was accompanied with the reduction of abnormal valence iron ( $\text{Fe}^{4+}$ ) site in the surface layer ( $< 300$  °C). The active oxygen species reversibly appeared and disappeared on the iron site due to the sorption of atmospheric oxygen at the same temperature range.

### Acknowledgments

Authors thank Prof. T. Hibino (Nagoya University) for enlightening advice. We are also grateful to Mr. S. Komai (Nagoya University) for his measurement of the Raman spectra.

### References

- [1] Y.M. Kang and B.Z. Wan, *Appl. Catal. A* 114 (1994) 35.
- [2] R.S. Drango, K. Jurczyk, D.L. Singh and V. Young, *Appl. Catal. B* 8 (1996) 405.
- [3] A. Musialik-Piotrowska, B. Mendyka and K. Syczewska, *Catal. Today* 11 (1992) 597.
- [4] S. Chatterjee and H.L. Greene, *J. Catal.* 130 (1991) 76.
- [5] B. Bendyka, A. Musialik-Piotrowska and K. Syczewska, *Catal. Today* 11 (1992) 241.
- [6] A.A. Klinghofer and J.A. Rossin, *Ind. Eng. Chem. Res.* 31 (1992) 241.
- [7] J.A. Rossin and M.M. Farris, *Ind. Eng. Chem. Res.* 32 (1993) 1024.
- [8] H. Muler, K. Deller, B. Despeyroux, B. Peldszus, P. Kammerhofen, W. Kuhn, R. Spielmannleitner and M. Stroger, *Catal. Today* 17 (1993) 383.
- [9] L. Becher and H. Forster, *J. Catal.* 170 (1997) 200.
- [10] R. Spinicci, M. Faticanti, P. Marini, S. De Rossi and P. Porta, *J. Mol. Catal.* 197 (2003) 147.
- [11] A. Rougier, S. Soiron, I. Haihal, L. Aymard, B. Taouk and J.-M. Tarascon, *Powder Technol.* 128 (2002) 139.
- [12] R. Auer, M. Alifanti, B. Delmon and F.C. Thyron, *Appl. Catal. B-Environ.* 39 (2002) 311.
- [13] A. Gil, L.M. Gandia and S.A. Korili, *Appl. Catal. A-Gen.* 274 (2004) 229.
- [14] W.W. Malinofsky and H. Kedesdy, *J. Amer. Chem. Soc.* 76 (1954) 3090.
- [15] S. Mori, *J. Amer. Ceram. Soc.* 49 (1996) 600.
- [16] J.C. Vázquez, F.M. Figueiredo, J.C. Waerenborgh, W. Zhou, J.R. Frade and J.T.S. Irvine, *J. Solid State Chem.* 177 (2004) 3105.
- [17] B.S. Randhawa and K. Sweet, *Bull. Mater. Sci.* 23 (2000) 305.
- [18] A.A. Davydov, M.P. Komarova, V.F. Anufrienko and N.G. Maksimov, *Kinet. Catal.* 14 (1973) 1342.
- [19] E. Giamello, S. Sojka, M. Che and A. Zecchina, *J. Phys. Chem.* 90 (1986) 6084.
- [20] A. Zecchina, G. Spoto and S. Coluccia, *J. Mol. Catal.* 14 (1982) 351.
- [21] S. Fujita, H. Nakano, K. Suzuki, T. Mori and H. Masuda, *Catal. Lett.* 106 (2006) 139.
- [22] S. Fujita, M. Ohkawa, K. Suzuki, H. Nakano, T. Mori and H. Masuda, *Chem. Mater.* 15 (2003) 4879.
- [23] K. Sato, J. Iritani, R. Miyamoto, S. Fujita, K. Suzuki, M. Ohkawa and T. Mori, *Stud. Surf. Sci. Catal.* 158 (2005) 2001.
- [24] Y. Jin and A.K. Datye, *J. Catal.* 196 (2000) 8.
- [25] A. Venugopal and M.S. Scurrell, *Appl. Catal. A Gen.* 250 (2004) 241.
- [26] P. Ciambelli, S. Cimino, S. De Rossi, L. Lisi, G. Minelli, P. Porta and G. Russo, *Appl. Catal. B* 29 (2001) 239.
- [27] J.C. Waerenborgh, F.M. Figueiredo, J.R. Jurado and J.R. Frade, *J. Phys., Condens. Mater.* 13 (2001) 8171.